



Lawton, MC., & McGeehan, JP. (1992). The application of GTD and ray launching techniques to channel modelling for cordless radio systems. In *IEEE 42nd Vehicular Technology Conf., Denver, May 1992* (Vol. 1, pp. 125 - 130). Institute of Electrical and Electronics Engineers (IEEE). <https://doi.org/10.1109/VETEC.1992.245457>

Peer reviewed version

Link to published version (if available):
[10.1109/VETEC.1992.245457](https://doi.org/10.1109/VETEC.1992.245457)

[Link to publication record on the Bristol Research Portal](#)
PDF-document

University of Bristol – Bristol Research Portal

General rights

This document is made available in accordance with publisher policies. Please cite only the published version using the reference above. Full terms of use are available:
<http://www.bristol.ac.uk/red/research-policy/pure/user-guides/brp-terms/>

The Application of GTD and Ray Launching Techniques to Channel Modelling for Cordless Radio Systems

M.C. Lawton and J.P. McGeehan
University of Bristol
Centre for Communications Research
Queens Building, University Walk
Bristol BS8 1TR, United Kingdom
Tel: +44 272 303727, Fax: +44 272 255265

Abstract

Propagation characteristics play a fundamental role in the design and implementation of radio systems. The application of broadband digital data services within the cordless environment requires close consideration of the dispersive nature of radio channels. A prediction algorithm is presented such that propagation characteristics can be estimated for small cell high data rate systems. Through the use of Geometric Optics and Geometric Theory of Diffraction (GTD) the algorithm performs ray launching techniques in order to evaluate reflected, transmitted, and diffracted rays from a simplified description of a given environment. Both modelled and measured results are presented demonstrating the model's ability to predict typical RMS delay spread values.

1 Introduction

The last decade has seen an unprecedented growth in the use of mobile and cordless radio systems, offering primarily voice communication. However, increasingly, work is now being directed towards digital data services. In addition, the success of mobile telephony has resulted in considerable interest in incorporating spectrally efficient small cell systems. For such systems the extent of the time dispersion and hence intersymbol interference provided by the channel becomes an important criterion limiting the data rate of the system. This paper considers the propagation characteristics of small cell high data rate systems. Rather than use a simulation approach an analytical ray launching technique has been developed. Ray launching techniques were initially used to model narrowband fading statistics by Gladstone and McGeehan [1], in both single and multi-transmitter mobile radio systems, and are

now becoming an increasingly attractive proposition for wideband modelling given the advances in computer technology and the trend towards smaller cells.

2 The Propagation Model

The equation used to describe the channel was first proposed by Turin [2] and has subsequently been used by several authors [3, 4]. It takes the form of a band-limited complex impulse response, $h(t)$, given by:-

$$h(t) = \sum_{k=1}^n \alpha_k \cdot \delta(t - \tau_k) \cdot \exp(j\Phi_k) \quad (1)$$

Here the transmitted pulse is mathematically described by a Dirac function and the received signal, $h(t)$, is formed from the addition of waves from several time delayed paths each represented by an attenuated and phase shifted Dirac waveform.

The method adopted in this paper directly seeks to evaluate suitable path parameters for the amplitude α_k , arrival time τ_k , and the arrival phase Φ_k , such that the propagation characteristics can be predicted. This calculation uses geometric optics and the geometric theory of diffraction.

2.1 Geometric Optics

The algorithm uses geometric optics in order to calculate analytically all reflected and transmitted paths up to and including seven reflections for an outdoor picocell application. This typically results in excess of one hundred and fifty rays.

Conceptually the algorithm works by reflecting the entire room plus receiver about a chosen reflecting wall.

A line is then drawn between the transmitter and receiver image. If this is intersected by the reflecting wall and no other walls then a purely reflected path is said to exist. The value of τ_k for this path is found from the length of the line and the speed of light. α_k is found by using a square law attenuation of signal power with distance and incorporating a reflection loss. Φ_k can be evaluated from the path length and knowledge of the carrier frequency with allowances being made for phase transitions resulting from reflections or diffraction.

In the event of the line between transmitter and reflected receiver being intersected by more than the intersecting plane then a path is said to exist but the wave is attenuated further by passing through a blocking wall or walls.

The basic idea for the algorithm can be extended to include any number of reflections. The reflection and transmission characteristics have been evaluated as a function of arriving angle for a range of different wall materials. The algorithm has also been made more realistic by giving both transmitting and receiving antenna gain patterns. Both antennas were modelled as vertically polarised half-wave dipoles.

Previous work has been reported by the authors [5] where the model was used for the prediction of radio channel characteristics for indoor cells. In such cells it was necessary to have a 3-D model such that multiple ceiling-floor reflections could be modelled. For the outdoor application described in this paper it was decided to adapt the model for a 2-D environmental description. In doing this an assumption is made that the transmitter height is below roof top height and therefore roof top dimensions need not be inputted. However whilst all the reflectors are described in terms of x and y the ground is still represented within the model. For each path found an additional path corresponding to the same path with an extra ground reflection is added. Hence receiver and transmitter heights are still needed as inputs to the model.

This simplification has resulted in a reduction in the maximum possible number of purely reflected rays for a given number of reflections within a simple empty environment. However the increased simplicity of the algorithm allows the program to calculate paths up to seven reflections as opposed to maximum of five for the indoor model.

2.2 Geometric Theory of Diffraction

The application of geometric optics provides a simple and effective method for predicting the behaviour of radio channels. The method is however approximate

and as such has limitations. For a non-LOS (line of sight) scenario geometric optics suffers from its exclusion of the diffracted ray paths. It was felt that in the frequency band considered here (centre frequency 1.845 GHz) the effect of the diffracted rays may well be significant and thus warranted investigation.

GTD owes its origins to Keller's attempts to improve on geometric optics and has been designed as an extension to a geometric optics approach. Thus the two methods can elegantly be combined to provide a single prediction tool. The formulation of diffracted paths is similar to that of reflected paths in geometric optics except that the reflection coefficient is replaced with a diffraction coefficient and alterations made to the spatial attenuation factor. Figure 1 shows the geometry for diffraction by a curved edge.

The diffracted field, for either soft (perpendicular) or hard (parallel) polarization, resulting from a finitely conducting wedge can be calculated without singularity problems at the incidence and reflection boundaries using [6]:-

$$D_s^h = \frac{-e^{(-j\pi/4)}}{2n\sqrt{2\pi\beta\sin\beta'_0}} \left\{ \cot\left[\frac{\pi+(\phi-\phi')}{2n}\right] F(\beta L g^+(\phi-\phi')) \right. \\ + \cot\left[\frac{\pi-(\phi-\phi')}{2n}\right] F(\beta L g^-(\phi-\phi')) \\ + R_{0\perp} \cot\left[\frac{\pi-(\phi+\phi')}{2n}\right] F(\beta L g^-(\phi+\phi')) \\ \left. + R_{n\perp} \cot\left[\frac{\pi+(\phi+\phi')}{2n}\right] F(\beta L g^+(\phi+\phi')) \right\} \quad (2)$$

where the *Fresnel transition function*,

$$F(x) = 2j\sqrt{x}e^{jx} \int_{\sqrt{x}}^{\infty} e^{-j\tau^2} d\tau \quad (3)$$

and

$$L = \frac{ss' \sin^2 \beta'_0}{s+s'} \quad (4)$$

$$g^\pm(k) = 2\cos^2\left(\frac{2n\pi N^\pm - k}{2}\right), \quad k = \phi \pm \phi' \quad (5)$$

In equation (5), N^\pm are the integers which most closely satisfy the equations :-

$$2\pi n N^+ - (k) = \pi \quad (6)$$

and

$$2\pi n N^- - (k) = -\pi \quad (7)$$

$R_{0\perp}$ and $R_{n\perp}$ are the reflection coefficients for the perpendicular and parallel polarization for the 0 face, incident angle ϕ' , and for the n face, reflection angle $n\pi - \phi$ (figure 1).

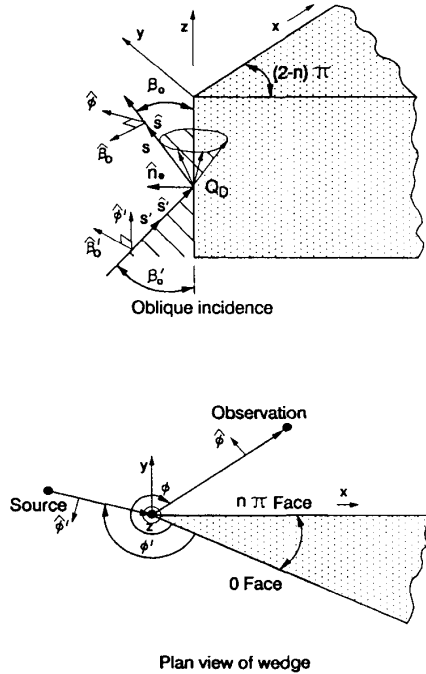


Figure 1: Geometry and co-ordinates for description of diffracted path at a wedge

Although the mathematical expressions for the diffraction terms look somewhat cumbersome and difficult to manipulate they can quite readily be evaluated by a computer. Calculation of the diffracted fields does however add further complexity to the algorithm and it was felt necessary to limit the computation performed. Consequently the algorithm described evaluates the first and second order diffraction terms along with all combinations of one reflection and one diffraction. For each diffracted path calculated the same path with an additional ground reflection is also evaluated.

2.3 Measurement Sites

Two measurement sites are described in this paper (see figures 2 and 3). The principal reflectors for each site are shown in heavy lines with shading used to represent buildings. These sites were chosen because it was felt that they represented two quite different cordless environments.

2.3.1 Site 1 (see figure 2)

This was the smaller site and was chosen because of its simplicity for description within the model and because it represented a confined linear cell. The transmitter was placed at the end of a roadway which provided the entrance to a large 'U' shaped building surrounding three of the entrance's four sides. The area behind the transmitter is a car park which offered many potential scatterers. Measurement of both LOS and obstructed (OBS) paths were taken. The environmental description within the model is also indicated on the map. Principal reflectors, diffraction points, receiver locations are all shown. The outer cell dimensions have been bounded by reflecting planes represented by thick solid lines. This was done because it was felt that for these antenna heights ($T_x = 2.5\text{m}$, $R_x = 1.5\text{m}$) it was more likely for dissipating rays to encounter obstacles than continue in free space.

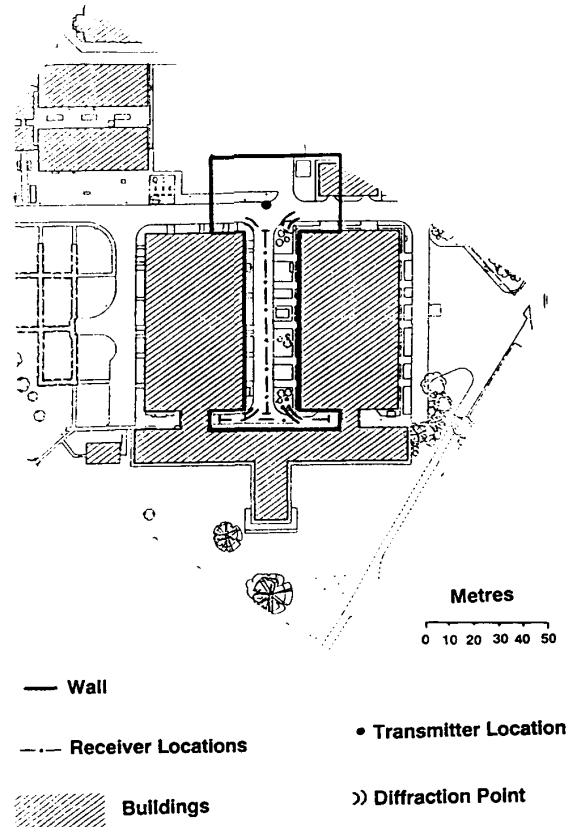


Figure 2: Environmental description for Site 1 (Heavy lines show representation of obstacles within the model)

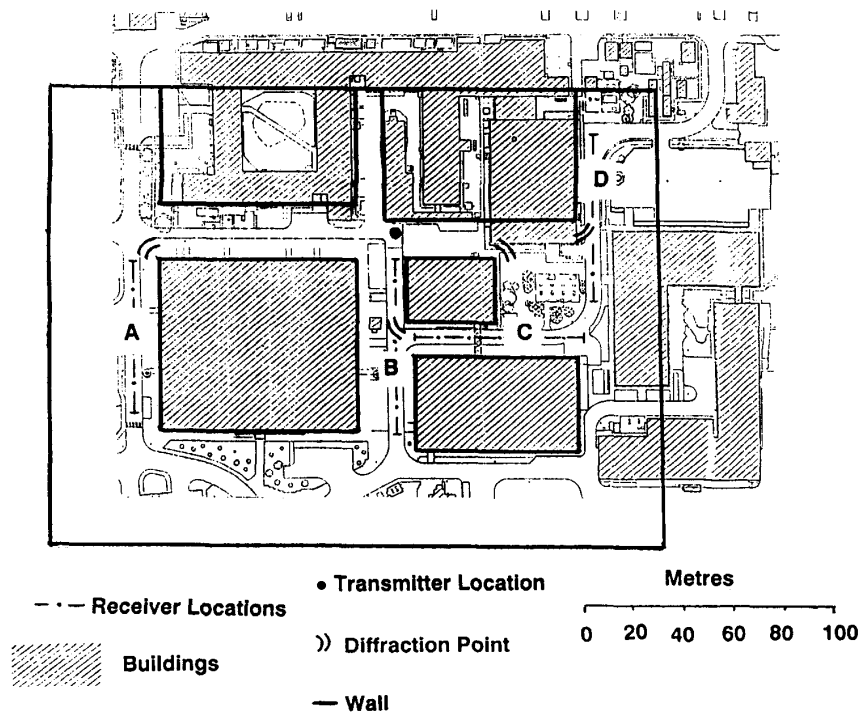


Figure 3: Environmental description for Site 2 (Heavy lines show representation of obstacles within the model)

2.3.2 Site 2 (see figure 3)

This area was chosen in an attempt to model a more complicated scenario which might be typical of a street location. A combination of both LOS and OBS profiles was measured along the four lines shown (A-D). Various simplifications have been made for the environmental description in the model in an attempt to combine high speed with a reasonably accurate model.

2.4 Measurements Undertaken

Care was taken that the measurement and modelling techniques should be as similar as possible. Many impulse responses were both measured and modelled at the receiver locations indicated on the maps. These were then used to generate power delay profiles and subsequently their *RMS delay spreads*[7] values were calculated. The RMS delay spread is a measure of the time dispersion of a transmitted pulse. The results were then presented as a cumulative distribution and both measured and modelled results compared.

For the measured results the receiver was kept stationary. This was done so that the sounder statistics would average over a stationary channel. Also it was felt that the limited Doppler information available (from a moving receiver) was not an important de-

sign criterion because for most systems the worst case Doppler shift would need to be assumed, and this is a parameter which is easily calculated.

3 Results

3.1 Wideband Modelling

Figure 4 shows a typical Doppler scattergrams for a location at site 2. Doppler scattergrams contain all the information represented within a power delay profile with additional Doppler information added. This clearly shows the ability of the algorithm to evaluate individual rays.

The cumulative distribution of the RMS delay spread values is shown in figures 5 and 6. The modelled and measured results agree quite closely in each case. The smaller RMS delay spread values were found in site 2 which was the smaller cell. Here there is a range between 40 nS and 130 nS with a median value of about 70 nS.

Whilst there is good agreement between modelled and measured results it is apparent that in both cases the modelled results have a lower maximum RMS delay spread value. This is probably because the model

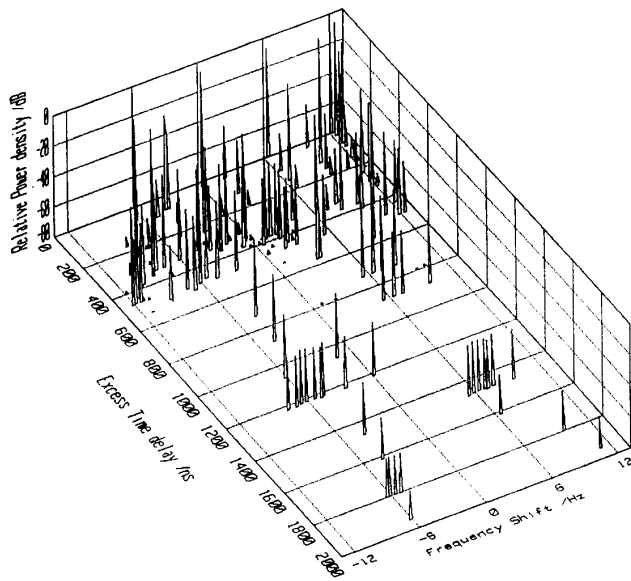


Figure 4: Doppler Scattergram for Site 1 with receiver positioned 40m from transmitter

confines the cell barriers at the outer perimeter and thus may fail to find the occasional distant reflected path.

In order to consider more closely the factors affecting RMS delay spread, the simple environment of site 1 was examined in more detail. The RMS delay spread was found for many positions as the receiver was moved along the path used in the measurements. These results were then compared with measured results at identical locations (see Figure 7). The graph indicates that the model is not able to predict localised low or high values. There would appear to be two principal reasons for this. Firstly, the model does simplify the channel with insufficient information to predict small scale details, i.e localised scattering from vehicles, humans etc. Secondly, the measurement device works with a finite bandwidth so that, unlike the model, it experiences multipath effects for rays arriving with very short time delays. The effect of this fading could have been reduced by performing the averaging with small scale movements of the transmitter. The model does however show that for this environment the RMS delay spread peaks at around 45m from the transmitter and is lower both close to the transmitter

and close to the building at the road end.

3.2 Narrowband Modelling

In addition to wideband characteristics of the radio channel, the narrowband characteristics have also been studied for both sites. Many signal strength values have been calculated for both LOS and OBS scenarios and their statistics have been studied. For the non-LOS case the signal strength values have been found to be well represented by the Rayleigh distribution and for the LOS case the amplitudes have been found to be well represented by the Rician distribution, with a varying K factor (the ratio of known/scattered powers). Close to the transmitter the K factor was found to be as high as 10 dB. For more distant LOS locations the K factor was found to be around 0 dB (see figure 8).

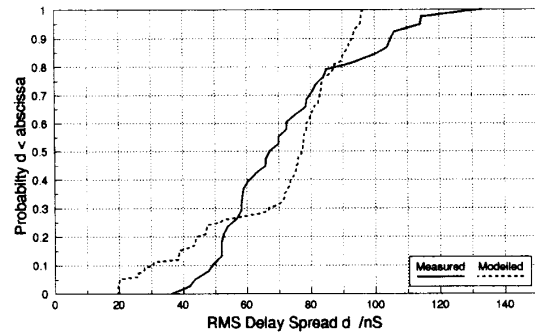


Figure 5: Modelled and measured RMS delay spread values for Site 1

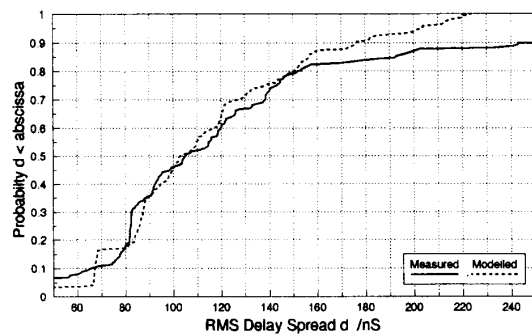


Figure 6: Modelled and measured RMS delay spread values for Site 2

4 Conclusions

A reflection and diffraction based algorithm has been shown to be a useful tool for the prediction of RMS delay spread values for two different outdoor environments. Previous work has shown the ability of a reflection based model to predict measured RMS delay spread values for indoor environments [5].

However the model cannot predict small scale fluctuations in the RMS delay spread.

The algorithm has also been used in order to simulate the narrowband behaviour of the two sites. For the obstructed (OBS) case the signal strength values are well represented by a Rayleigh distribution. For the line of sight (LOS) the results were modelled by a Rician distribution with varying K factors depending on the transmitter-receiver separation.

5 Acknowledgements

The authors would like to thank SERC and BT labs for the award of a SERC CASE research studentship. In addition they are grateful to BT for the provision of their channel sounding and laboratory facilities, and in particular, they wish to acknowledge the assistance of Paul Tattersall, Head of Mobile Propagation Group, for his contributive comments to the research programme. Finally the authors are indebted to their colleagues in the Centre for Communications Research, University of Bristol for the valuable advice and comments, and the provision of computing facilities.

References

- [1] K. J. Gladstone and J. P. McGeehan, "A Computer simulation of the Effect of Fading on a Quasi-Synchronous Sideband Diversity AM Mobile Radio Scheme," *IEEE Trans. on Selected areas of Comms*, vol. SAC-2, pp. 191-203, January 1984.
- [2] G. L. Turin, F. D. Clapp, T. L. Johnston, S. B. Fine, and D. Lavry, "A Statistical Model for Urban Multipath Propagation," *IEEE Trans. Vehicul. Technol.*, vol. VT-21, pp. 1 - 9, February 1972.
- [3] H. Suzuki, "A Statistical Model for Urban Radio Propagation," *IEEE Trans. Vehicul. Technol.*, vol. VT-40, pp. 203 - 210, July 1991.
- [4] R. Ganesh and K. Pahlavan, "Statistical modelling and computer simulation of indoor radio channel," *IEE Proc. I.*, vol. 138, pp. 153 - 161, June 1991.
- [5] M. C. Lawton, R. L. Davies, and J. P. McGeehan, "An analytical model for indoor multipath propagation in the picocellular environment," *6th Int. Conf. on Mobile Radio and Personal Comms, Warwick, UK*, pp. 1- 8, December 1991.
- [6] R. J. Leubbers, "Finite Conductivity Uniform GTD Versus Knife Edge Diffraction in Prediction of Propagation Path Loss," *IEEE Trans. Antenn. Propag.*, vol. AP-32, pp. 70 - 76, January 1984.
- [7] D. C. Cox, "Delay Doppler Characteristics of Multipath Propagation at 910 MHz in a Suburban Mobile Radio Environment," *IEEE Trans. Antenn. Propag.*, vol. AP-20, pp. 625 - 635, September 1972.

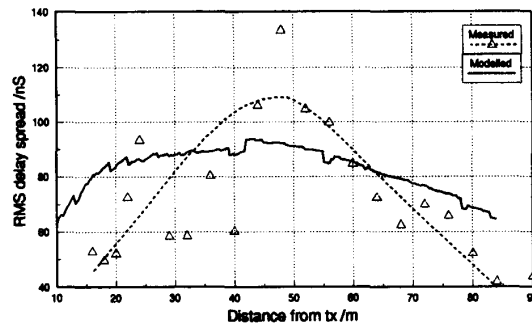


Figure 7: Modelled and measured variation in RMS delay spread with distance from the transmitter for Site 1

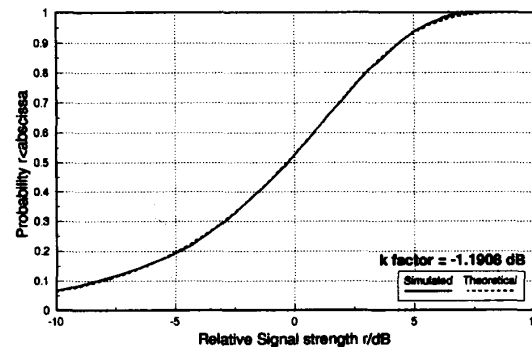


Figure 8: Rician statistics in Site 1 for a LOS case with receiver-transmitter separation = 40m